Electronic Supplementary Material (ESI) for Physical Chemistry Chemical Physics.
This journal is © the Owner Societies 2015

SUPPLEMENTAL INFORMATION: REACTIVE AND UNREACTIVE PATHWAYS IN A PHOTOCHEMICAL RING OPENING REACTION FROM 2D FEMTOSECOND STIMULATED RAMAN

*David T. Valley[1], David P. Hoffman[2] and Richard A. Mathies**

Department of Chemistry, University of California Berkeley, Berkeley, California 94720, United States

---

*To whom correspondence is addressed
E-mail: ramathies@berkeley.edu
Phone: (510) 642-4192

[1] Current address: Department of Chemical Engineering and Material Science, University of Minnesota – Twin Cities, 421 Washington Ave SE Minneapolis, MN, 55455, United States

[2] Current address: Janelia Research Campus, Howard Hughes Medical Institute, Ashburn, Virginia 20147, United States

Actinic pump – Raman probe cross correlation

Figure S1 presents the cross-correlation between the 560 nm centered actinic pump and NIR Raman probe beams as measured by the optical Kerr effect in pure solvent. This measurement was used to determine zero delay and the temporal resolution for the impulsive transient absorption experiments. The average FWHM for the actintic-probe interaction for the experiments measured was 75 fs with a total chirp of 10 fs in the probe beam.

Femtosecond Stimulated Raman

Figure S2 presents the excited state FSRS traces for ModCHD excited at 560 nm for time delays between 0 and 100 ps. The data shown is baseline corrected, with solvent features removed. Select traces of the data shown here comprise the excited state data shown in main text Figure 3.

Figure S3 presents the intensity-frequency trajectories between 0.2 and 2.0 ps for modes not included in main text Figure 6. The figure displays the intensity and frequency data for the 404, 509, 613, 905, 958, 1025, 1061, 1125, 1181, 1229, 1290, 1389, 1495, and 1505 cm^{-1} excited state peaks at high time resolution.

Figure S4 presents a correlation diagram for the 21 observed excited state FSRS peaks and the impulsively excited low frequency modes that modulate them. This figure differs from main text Figure 8 in that the oscillatory amplitudes listed are only corrected to reflect the magnitude at t=0. In this figure the area of the circle indicates the observed magnitude of the low frequency oscillatory signal. In fitting the oscillatory signal with damped sinusoids, the phase information was also retained. For this manuscript we have chosen not to include this information because of uncertainty introduced in the phase in the back extrapolation to the initial excitation, however we expect that phase information could provide valuable molecular information for future experiments evaluating impulsively driven FSRS oscillations. As a general trend for ModCHD we observe an initial redshift upon excitation for modes coupled to the 191cm^{-1} methyl twist and an initial blue shift for modes coupled to the 66 and 104 cm^{-1} frame bends.

The numeric data from Figure S4 as well as the main text figure 7 are presented in Table S1. For the FSRS modes indicated the table displays the frequency of oscillation (ISRS shift) as well as the normalized relative amplitude of oscillation (in %) and the absolute frequency amplitude in the oscillations (in cm^{-1}).

Figure S5 presents a purely Fourier analysis based approach to displaying the excited state oscillatory signal presented in main text Figure 8. The Fourier power spectra for the 467, 992, 1181, 1333, 1389, and 1580 cm^{-1} excited state stimulated Raman modes are displayed. The spectra are offset by their Raman shift, showing the amplitude of oscillatory components. For comparison the 200 fs SRS spectrum and ISRS spectrum are shown on the axes. From the Fourier representation of this data all of the peaks found using the LPSVD fit model of decayed sinusoids are also present. Further fitting would be necessary to extract physically relevant information from the Fourier approach.

Resonant Raman intensity analysis

To calculate the absolute displacement of the excited state Raman modes for ModCHD we evaluated the system using the time dependent resonant Raman formalism developed by Meyers and coworkers[1]. Resonant Raman spectra were taken with the 514 nm line of an Ar^{+} ion laser (Spectra Physics 2020). The beam was focused into a flowing dilute ModCHD cyclohexane solution through a capillary, and the scattered light was collected off axis and polarization selected, dispersed through a double grating spectrometer and detected with a cooled, back-illuminated CCD (LN/CCD-1100/PB; Roper Scientific).

Figure S6 presents the ModCHD extinction spectra and the simulated extinction spectra. The time dependent model was fit to the extinction spectra for closed ModCHD using home-written Raman intensity analysis code. The homogeneous broadening was set to reflect the fastest time decay constant observed for ModCHD (~500 fs), E0, the value of the 0-0 transition was set to the frequency where the absorption and emission spectra crossed (15700 cm^{-1}), and the relative displacements were taken from the intensities of a 514 nm resonant Raman spectrum where $I = \Delta^2\omega^2$. For the lowest frequency ModCHD modes (33, 66, and 104 cm^{-1}) displacements were determined by matching the relative intensity of the impulsive TA reconstructed spectra and calculating starting Δ values. The absolute displacements were determined by scaling the relative Δ values to match the extinction spectra, then the simulated spectrum was broadened using reasonable inhomogeneous broadening (650 cm^{-1}).

Figure S7 presents the resonant Raman spectra for ModCHD at 514 nm excitation, with the attached impulsive transient absorption frequency reconstructed spectra for the low frequency portion of the spectrum. The intensities for the low frequency region are scaled to match the intensity of the overlapping 191 cm^{-1} mode from the resonant Raman. The displacements obtained from fitting using the time dependent resonant Raman model are listed on top of the modes. The biggest Δ values correspond to the low frequency molecular bends at 4.5 and 2.0, the 191 cm^{-1} methyl wag at 1.0, the 509 cm^{-1} C=C-C=C torsion at 0.8 and the 1503 cm^{-1} C=C stretch at 0.95. For comparison, in 1-3 cyclohexadiene the C=C stretch is at 1578 cm^{-1} has a Δ value of 1.7[2].

DFT simulated Raman and resonant Raman.

Figure S8 presents the DFT optimized geometries for the ModCHD closed and ModCHD open ring configurations. These geometries were used to construct the reactive coordinate used in Figure 9 of the main text.

Figure S9 presents the DFT calculated pre-resonant, S1 resonant, and S2 resonant Raman spectra. These are compared to the experimental stimulated pre-resonant Raman, stimulated excited state Raman, and excited state impulsive transient absorption reconstruction spectra. For the three DFT simulated spectra the frequencies are all calculated from the ground state (scaled by 0.977), with different methods used to calculate the peak intensities and broadened by 7 cm^{-1}. The pre-resonant Raman intensities were calculated from the ground state polarizability derivatives. The S1 and S2 resonant Raman intensities were determined from the excited state nuclear forces and were calculated using TDDFT methods[3]. The S1 and S2 resonant Raman intensities were the primary source for the assignments on the excited state stimulated Raman.

Figure S10 is a control experiment to explore the possibility the generation of oscillatory signal of in ModCHD from 3rd order Raman cascades between the excited state ModCHD and non-resonant components in the solution. The cyclohexane data collected concurrently with that of the ModCHD presented in the main text was analyzed in similar manner. However, the cyclohexane data does not reveal any oscillatory signals. The spike present around zero delay is from interaction between the actinic pump and the Raman pump.

Figure S11 presents a comparison between the oscillatory intensity from the cyclohexane solvent 801 cm^{-1} peak and the ModCHD 1580 cm^{-1} peak. The oscillatory component extracted from the ModCHD 1580 cm^{-1} peak has maximum frequency amplitude more than 300 times greater than cyclohexane.

References

1. Meyers, A., B. & Mathies, R. A. in *Biol. Appl. Raman Spectrosc. Vol 2 - Reson. Raman Spectra Polyenes Aromat.* 1–58 (1987).

2. Trulson, M. O., Dollinger, G. D. & Mathies, R. A. Femtosecond photochemical ring opening dynamics of 1,3-cyclohexadiene from resonance Raman intensities. *J. Am. Chem. Soc.* **109,** 586–587 (1987).
3. Guthmuller, J. & Champagne, B. Time dependent density functional theory investigation of the resonance Raman properties of the julolidinemalononitrile push-pull chromophore in various solvents. *J. Chem. Phys.* **127,** 164507 (2007).

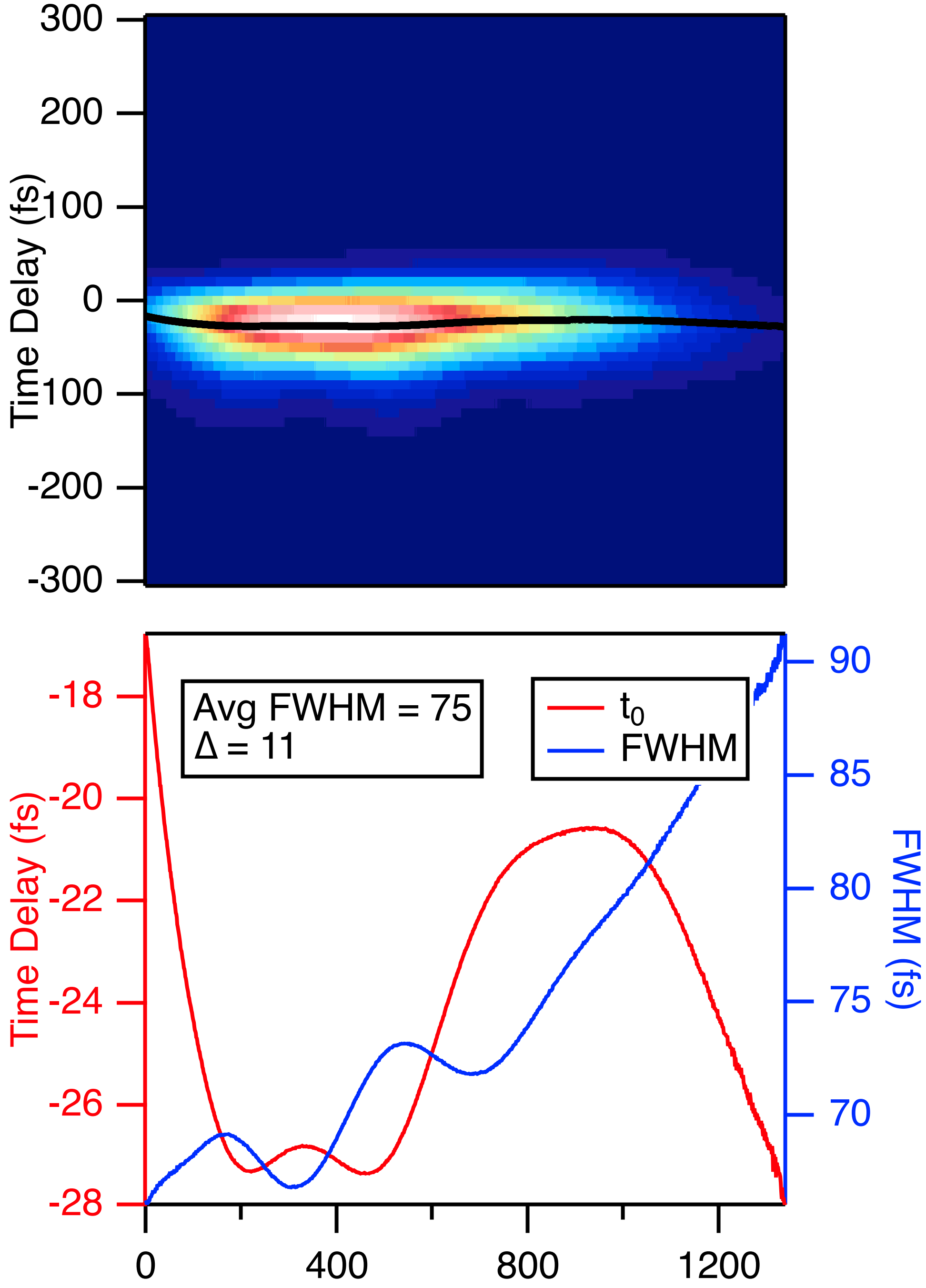

Figure S1: Frequency resolved optical Kerr effect cross correlation traces between actinic and probe pulses in flowed cyclohexane versus detector pixel. The figure below shows the fit peak center and full width half max for the cross correlation across the detector.

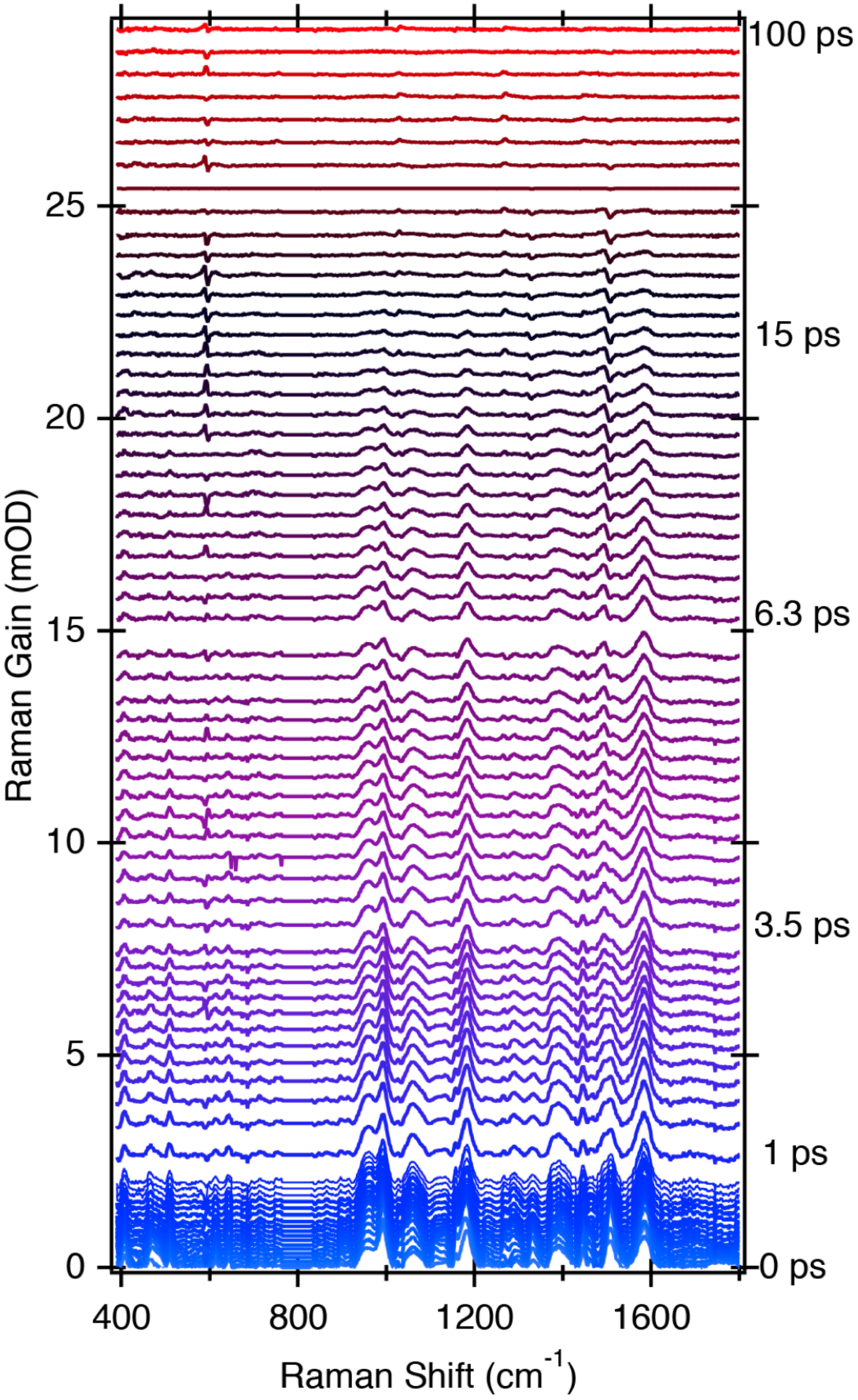

Figure S2: Selected excited state stimulated Raman spectra of ModCHD for time delays between 0 and 100 ps. The Data is spaced roughly logarithmically with time.

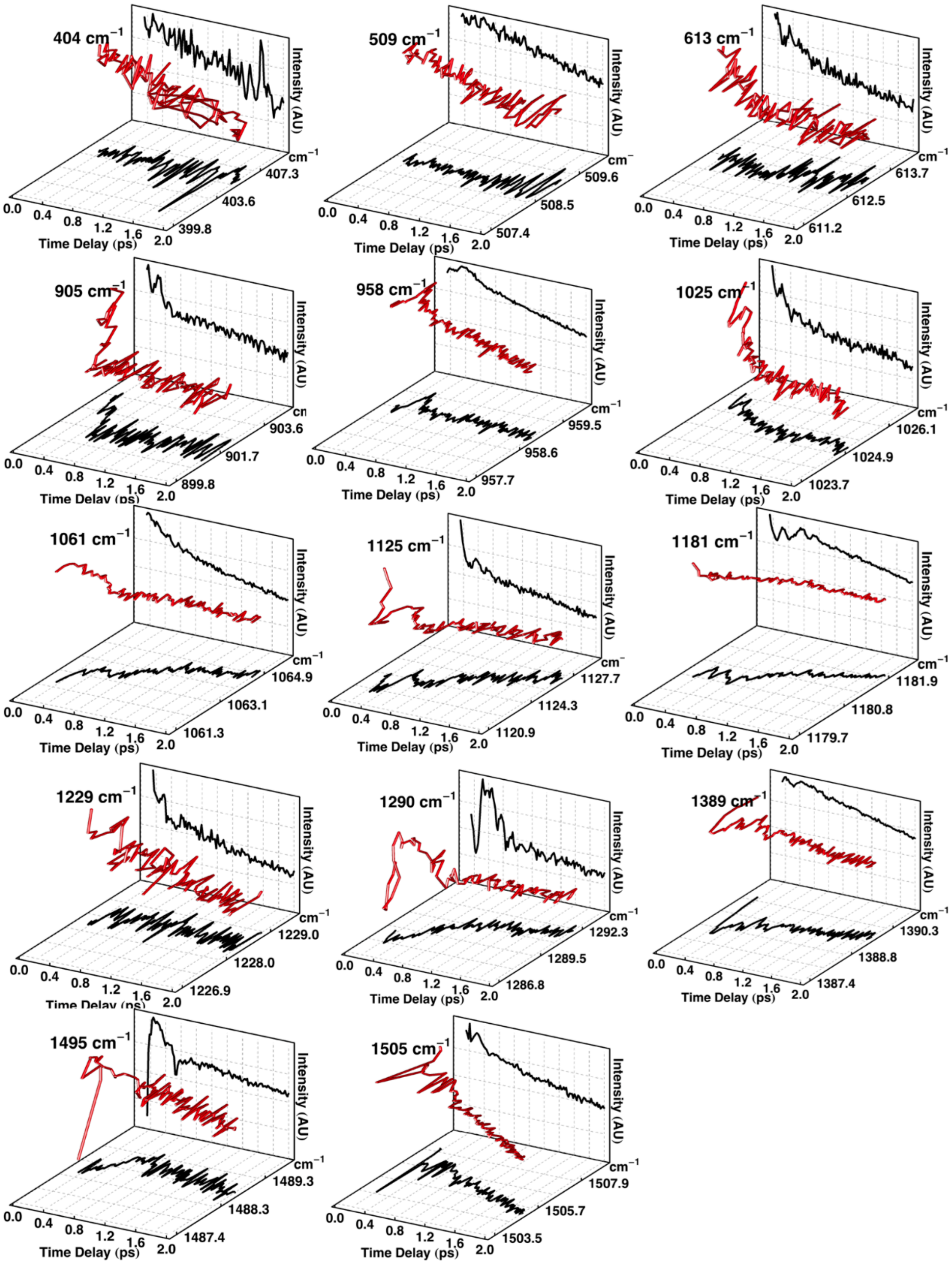

Figure S3: Intensity-frequency trajectories for the 404, 509, 613, 905, 958, 1025, 1061, 1125, 1181, 1229, 1290, 1389, 1495, and 1505 cm^{-1} excited state peaks of ModCHD. Each plot shows the peak's Raman shift and intensity at 20 fs intervals. Peak parameters were extracted using a Lorenztian lineshape model. Projections of the intensity and Raman shift are shown behind and below, respectively.

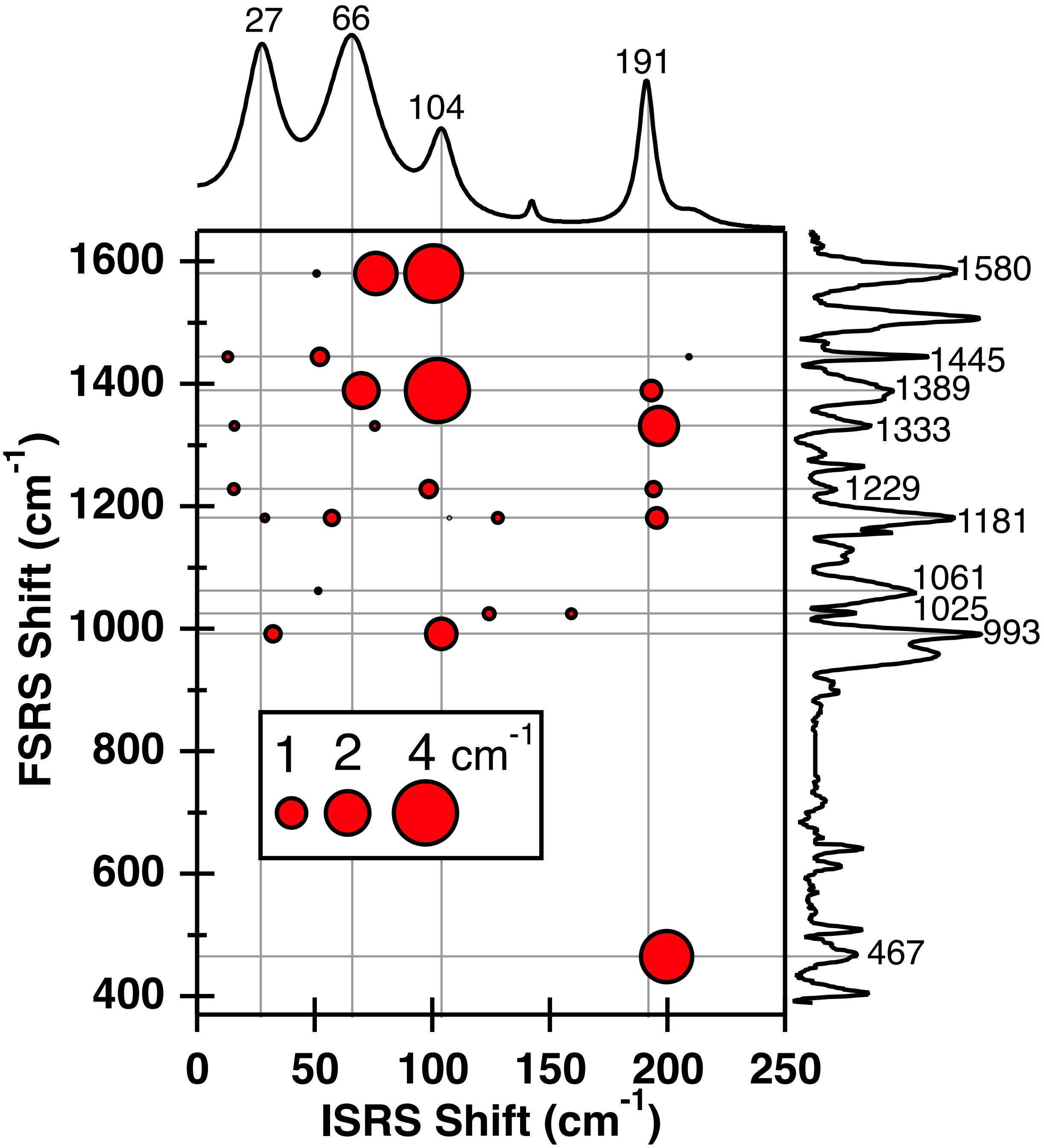

Figure S4: Correlation diagram between excited state FSRS modes and low frequency impulsive stimulated Raman modes. A stimulated Raman spectrum of the excited state of ModCHD at 200 fs delay is shown at right. The excited state ISRS spectrum from Figure 2(d) is shown at top. The circles' ordinates and abscissas indicate FSRS average frequency and FSRS peak center oscillation, respectively. The areas of the circles represent the observed oscillatory motion extrapolated to t=0.

FSRS Shift	ISRS Shift	Normalized ($\Delta\omega/\omega_0$)	Absolute (cm^{-1})
467	199.51	16.14	2.71
993	32.10	0.23	0.33
993	103.78	1.89	1.05
1181	28.73	0.05	0.11
1181	57.09	0.21	0.29
1181	107.17	0.03	0.02
1181	127.87	0.22	0.18
1181	195.40	0.69	0.49
1333	15.72	0.04	0.13
1333	75.48	0.12	0.12
1333	196.33	2.67	1.60
1389	69.70	0.73	1.38
1389	102.16	2.82	4.04
1389	193.07	0.42	0.48
1444	13.00	0.05	0.16
1444	52.15	0.32	0.36
1444	208.99	0.09	0.05
1580	50.78	0.03	0.07
1580	75.94	0.93	1.87
1580	100.43	1.99	3.27

Table S1: A table of the oscillations observed in the time-dependent FSRS data indicated in main text Figure 7 and SI Figure S4.

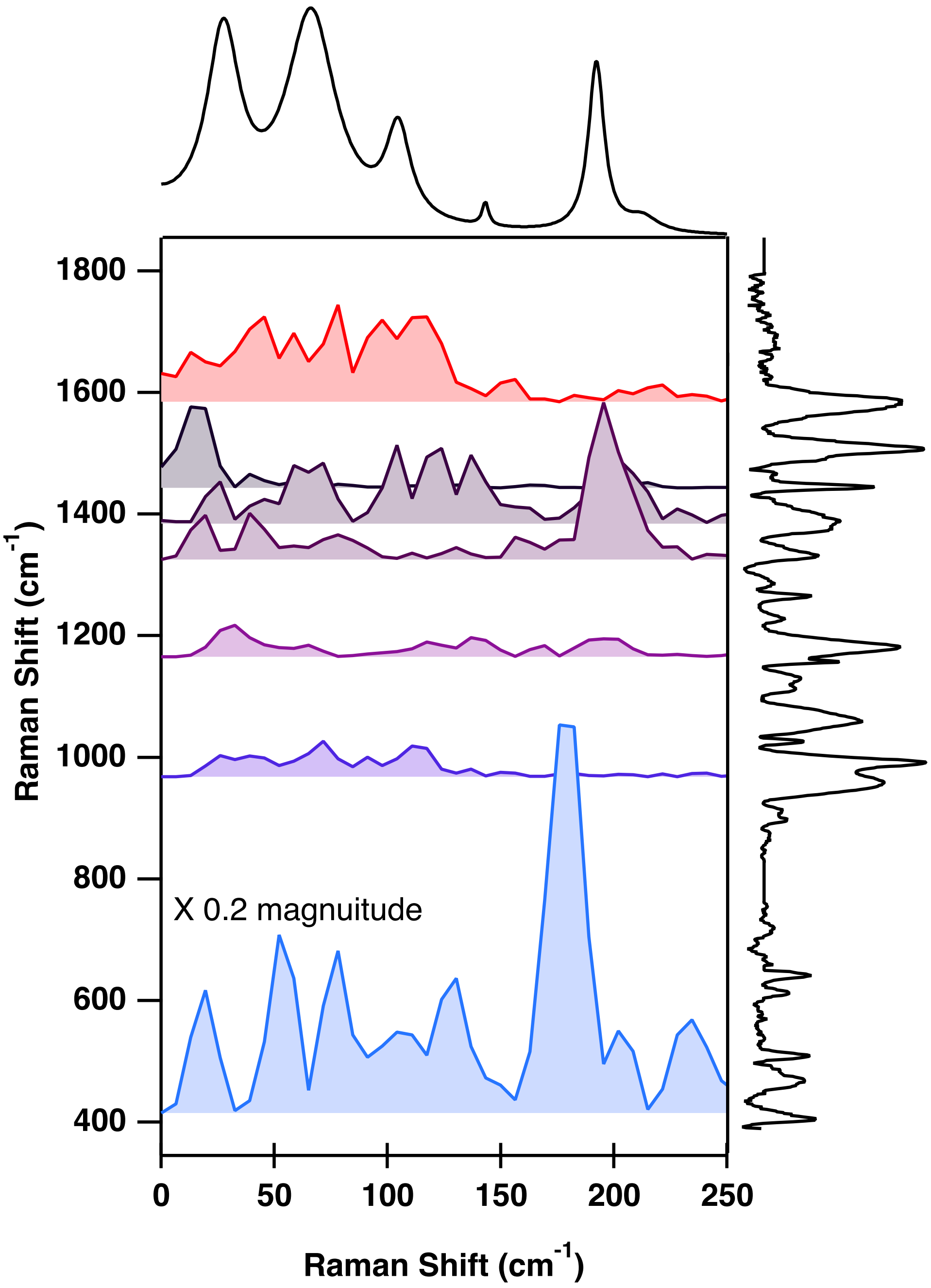

Figure S5: Fourier power spectrum correlation diagram between excited state FSRS modes and low frequency impulsive stimulated Raman modes. The frequency domain power spectrum for selected excited state FSRS modes is shown, with the baseline of the power spectrum curve corresponding to the excited state Raman shift and the frequency of the signal shown in vertical offset.

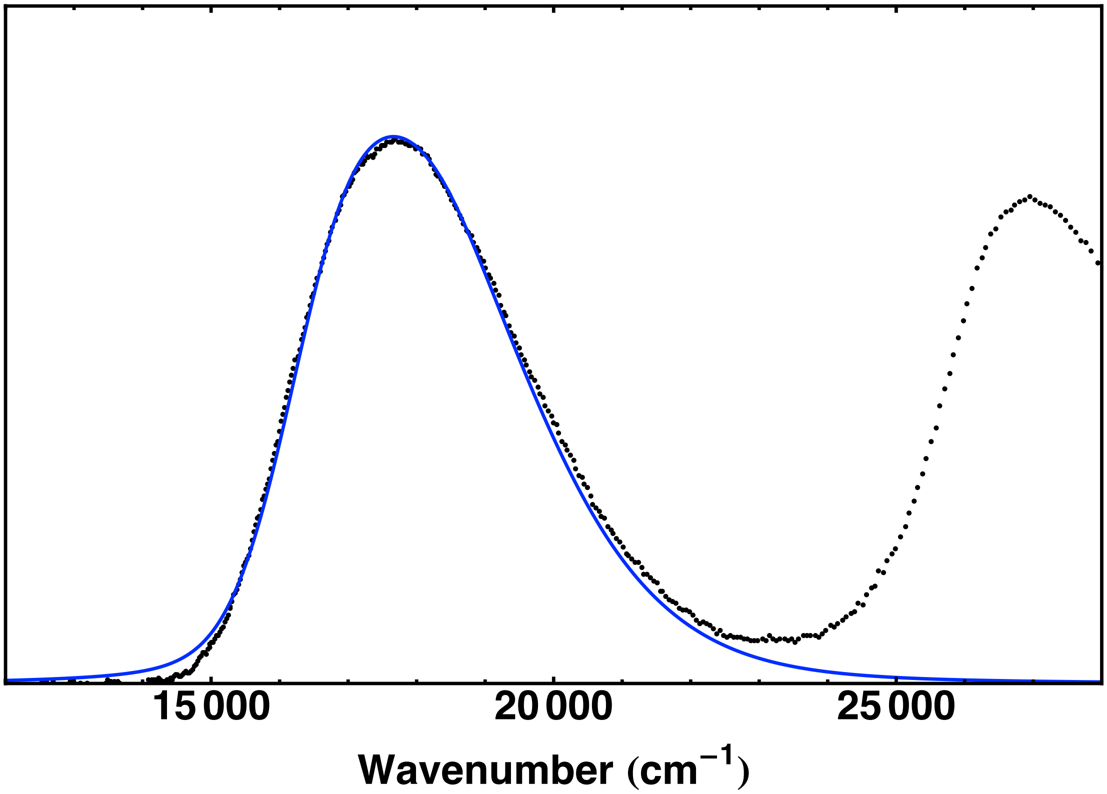

Figure S6: Extinction spectra of ModCHD (black) and simulated extinction spectra using the time dependent model from resonant Raman intensities (blue)

.

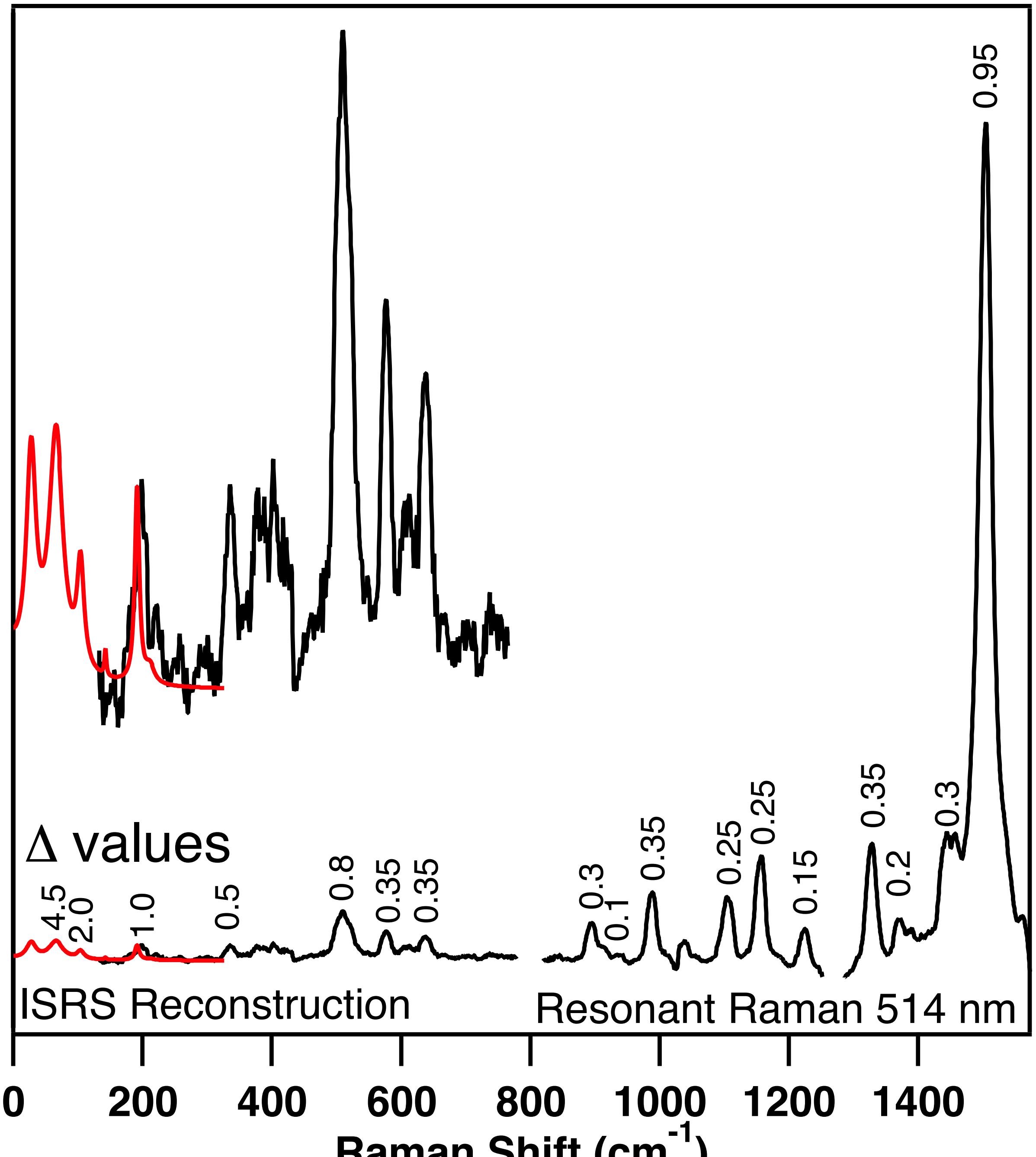

Figure S7: 514 nm Resonant Raman spectrum for ModCHD in cyclohexane (black) with solvent features removed and scaled ES ISRS spectra (red) included to approximate the low frequency portion of the spectra. Above presents the low frequency section of the spectrum scaled. The delta values shown are calculated by time dependent resonant Raman intensity analysis.

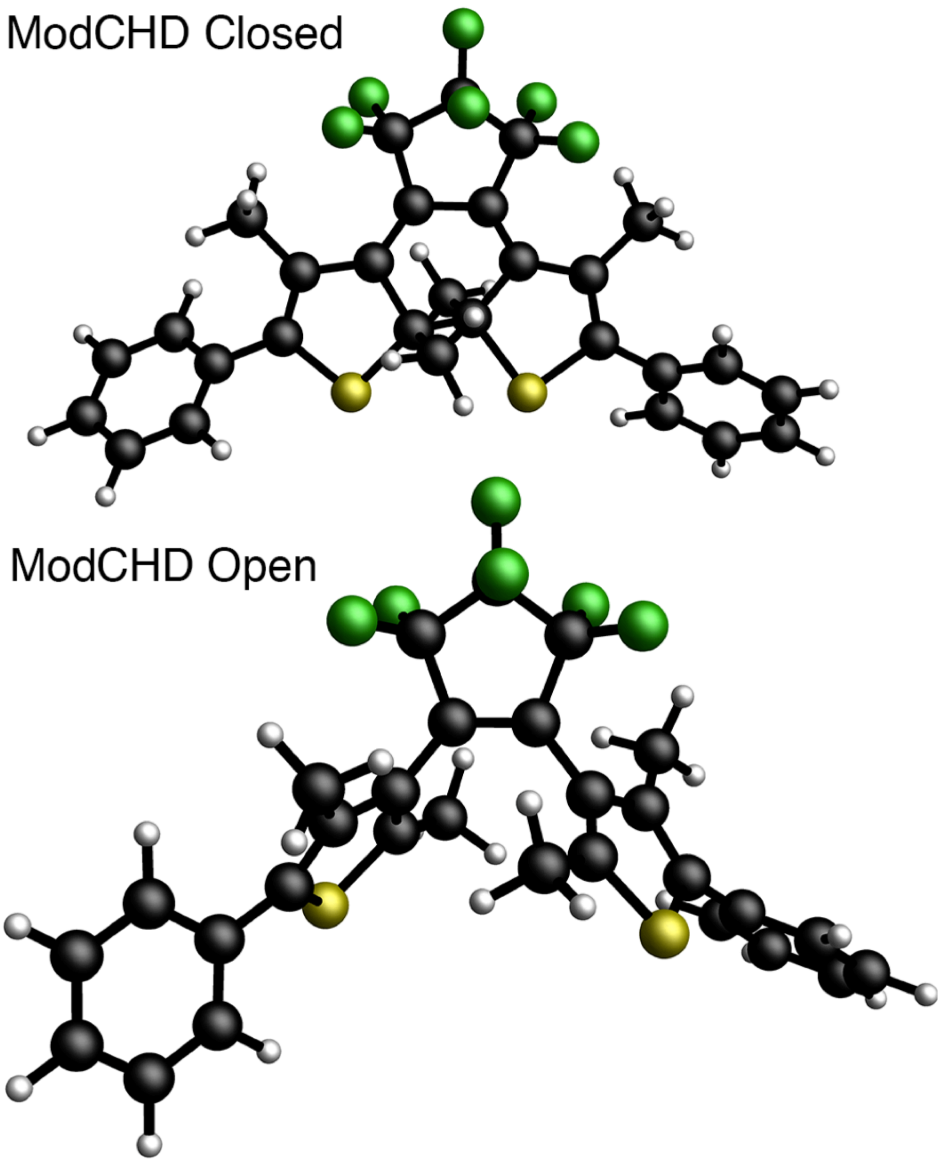

ModCHD Closed

ModCHD Open

Figure S8: Optimized geometry for ModCHD closed and open simulated using DFT (B3LYP functional at 6-311 ++ g (d,p) basis).

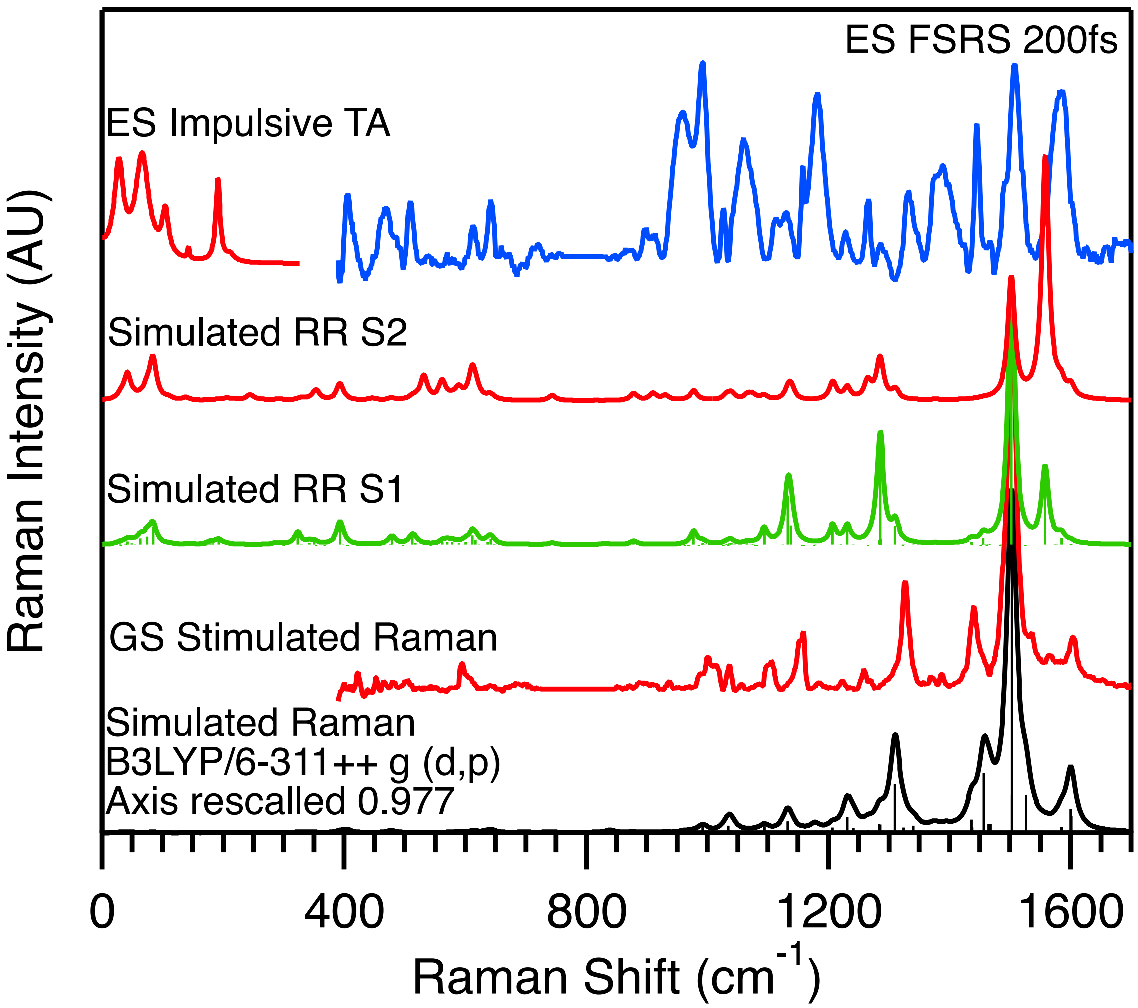

Figure S9: Bottom trace shows stick and broadened DFT calculated pre-resonant Raman spectra calculated for ModCHD with B3LYP functional at 6-311 ++ g (d,p) basis. The Raman shift axis for DFT Raman has been multiplied by a factor of 0.977. The ground state stimulated Raman is shown in the red trace. The ground state stimulated Raman spectrum is in red. Raman spectra resonant with S1 and S2 transitions were calculated from the forces of the excited state potential energy surfaces along the ground state normal modes. The top traces show the excited state impulsive transient absorption reconstructed spectrum and excited state FSRS at 200 fs.

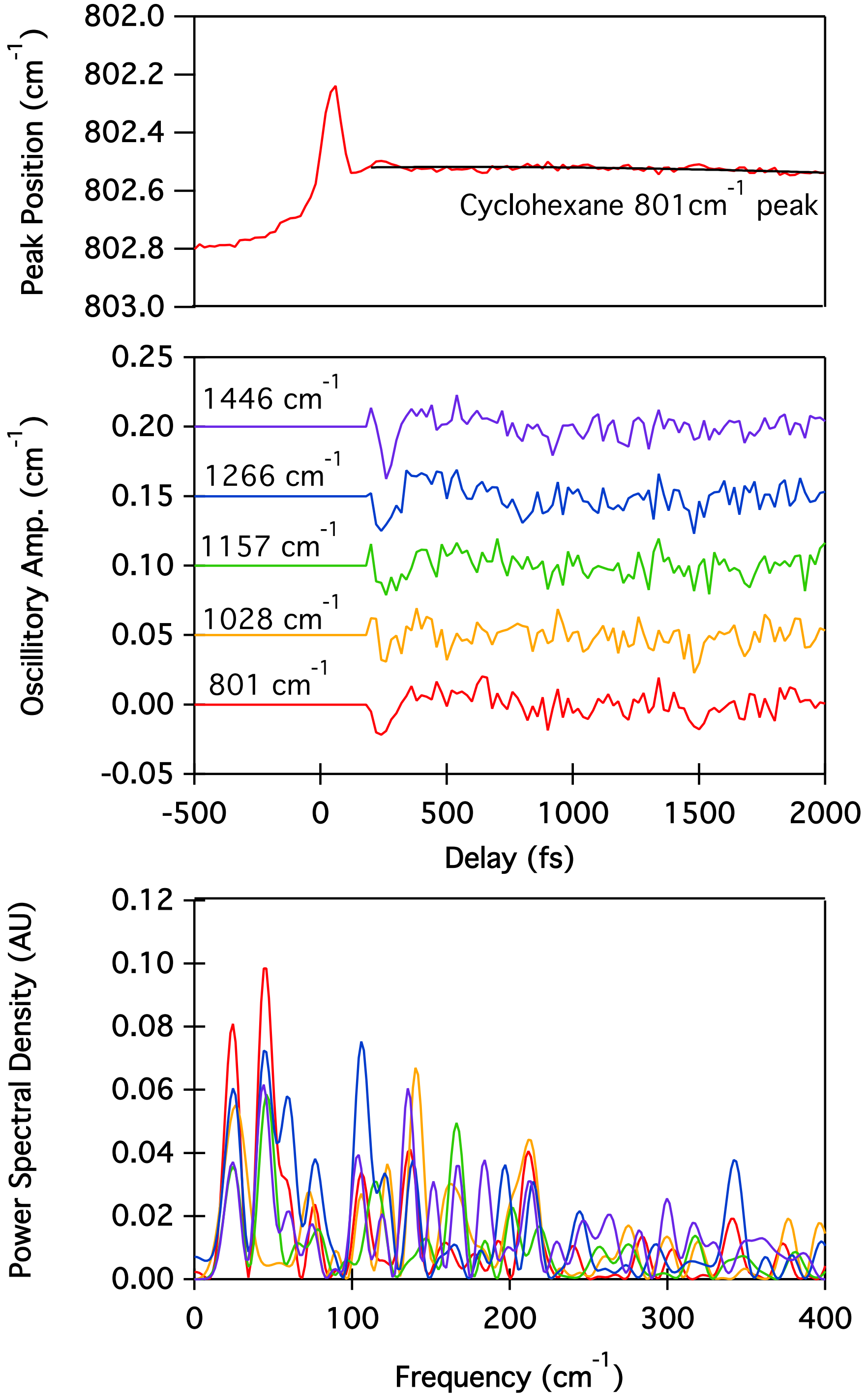

Figure S10: Cyclohexane peaks are analyzed in the same way as the ModCHD peaks to probe for the possibility of cascades. Top: Time trace for 801 cm^{-1} cyclohexane peak center and fit used to remove the kinetic response. Middle: Fit residual for five cyclohexane peaks - none show any oscillatory features with amplitude above 0.02 cm^{-1}. Bottom: FFT power spectra density from the five cyclohexane Raman peaks shows no clear oscillatory features. LPSVD algorithm did not detect any oscillatory signal from cyclohexane.

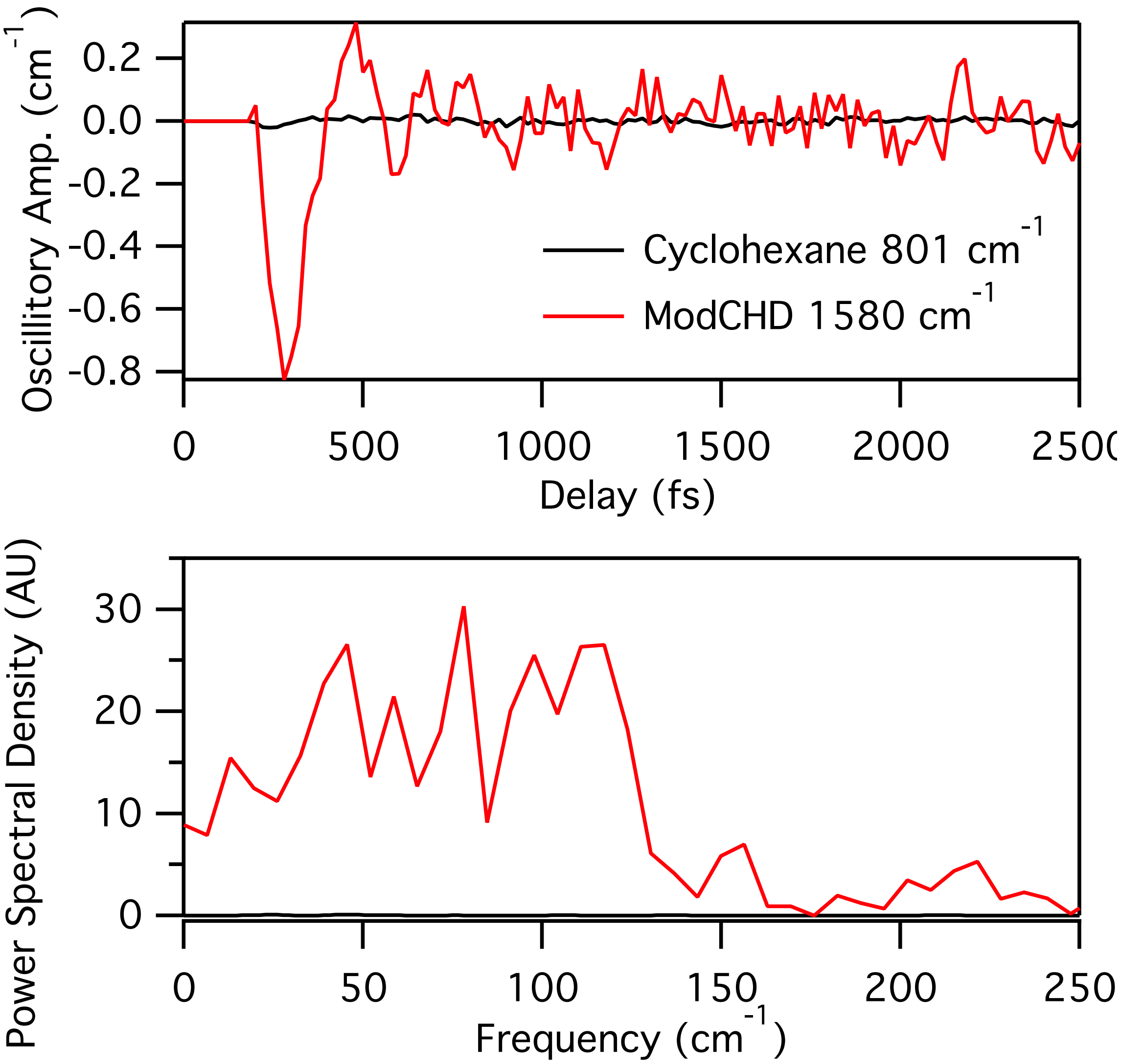

Figure S11: Comparison of oscillatory magnitude between the excited state ModCHD 1580 cm^{-1} and the Cyclohexane 801 cm^{-1} peak.